Experiments in Fluids 17 (1994) 330–336 © Springer-Verlag 1994

A combined OH/acetone planar laser-induced fluorescence imaging technique for visualizing combusting flows

B. Yip, M. F. Miller, A. Lozano, R. K. Hanson

Abstract A combined OH/acetone planar laser-induced fluorescence (PLIF) imaging technique that provides simultaneous visualizations of regions of unburned fuel and of combustion in a reacting flow is described. OH marks the location of chemical reaction and of combustion products, and acetone vapor, which is seeded into the fuel stream, marks unburned fuel. A single pulse from an ultraviolet laser is used to simultaneously excite both the OH and acetone, and the fluorescence from each is detected on separate cameras. Acetone spectroscopy and chemistry are reviewed to provide a basis for interpreting acetone fluorescence signals in high-temperature combusting environments. The imaging technique is applied to two nonpremixed turbulent reacting flows to assess the utility of the technique for visualizing the instantaneous flow structure and to illustrate the dependence of the interpretation of the acetone PLIF images on the flow conditions.

1 Introduction

Insights into the manner in which fuel and oxidizer mix and burn in nonpremixed turbulent reacting flows can be gained by studying their instantaneous structure. Planar laser imaging techniques (Hanson 1988) are well suited for investigating flow structure because they provide a time-resolved, two-dimensional map of a chosen flow variable (e.g., species number density). In particular, planar laser-induced fluorescence (PLIF) imaging of OH has been used widely because high signals are easily attainable and because OH is naturally present in many of the combusting flows of interest. However, OH measurements only provide information about regions of the flow where combustion has occurred.

A better understanding of the mechanisms of mixing and combustion in a reacting flow can be obtained if information about both reacting and nonreacting regions can be obtained simultaneously. Experiments where two detectors were employed to simultaneously visualize different flowfield properties in flames have been reported previously (Long et al. 1985, Dibble et al. 1986, Namazian et al. 1988, Schefer et al. 1990). While these visualization techniques yielded good results, they may not be easily applicable in larger flames or enclosed combustors. In such facilities, where the signals from Rayleigh scattering, Raman scattering or C_2 fluorescence may be too weak relative to background scattering or fluorescence, a more practical diagnostic which produces larger signals is needed.

Recently, acetone and acetaldehyde have been demonstrated as fluorescent tracer molecules in nonreacting flows and flames, and strong signals were obtained (Lozano et al. 1992, Arnold et al. 1990, Tait and Greenhalgh 1992). These large molecules exhibit a broadband UV absorption feature which overlaps the (0, 0), (1, 0) and (3, 0) vibrational bands of the $A \leftarrow X$ system of OH, all of which have been used for OH laser-induced fluorescence (LIF) measurements. Thus, a single UV laser can be used to simultaneously excite fluorescence from the fuel stream tracer molecule and from OH. Since OH fluoresces in the UV and acetone and acetaldehyde fluoresce in the visible, optical filtering can be used to separate the signals.

This paper presents a combined OH/acetone PLIF imaging technique which provides simultaneous, time-resolved visualizations of regions of combustion and of unburned fuel. OH marks regions of combustion, and acetone, which is seeded into the fuel stream, marks regions of unburned fuel. The technique offers the significant practical advantages that only one laser is required to excite both the OH and the acetone, and the signal levels are high. Additionally, acetone is an attractive fuel stream tracer since it is relatively inexpensive and nontoxic and high seeding levels are possible. These qualities make the application of this technique to large facilities possible. The spectroscopy of acetone and its chemical behavior in high-temperature environments is discussed in order to establish a basis for interpreting acetone PLIF images. Since OH imaging is a well-established combustion diagnostic and extensive documentation exists in the literature, it will not be discussed in detail here. The combined OH/acetone technique is demonstrated in a low-speed methane flame and in a supersonic, hydrogen-air mixing layer.

2 Acetone spectroscopy and chemistry

The acetone molecule (CH_3COCH_3) displays an electronic structure characteristic of the carbonyl group, with a singlet

Received: 13 October 1993/Accepted: 10 May 1994

B. Yip, M. F. Miller, A. Lozano, R. K. Hanson
High Temperature Gasdynamics Laboratory,
Mechanical Engineering Department, Stanford University,
Stanford, CA 94305, U.S.A.

Correspondence to: M. F. Miller

Support was provided for this work by the Air Force Office of Scientific Research, Aerospace Sciences Directorate, with Julian Tishkoff as Technical Monitor, and is gratefully acknowledged. The contributions of Mr. T. C. Island in operating the supersonic flow facility are also greatly appreciated.

ground electronic state S_0, a first excited singlet state S_1 and a corresponding excited triplet state T_1 at slightly lower energy. Acetone, which has a broadband absorption feature extending from 225 to 320 nm, can be promoted from S_0 to S_1 by ultraviolet excitation, and the excited singlet emits a blue broadband fluorescence between 350–550 nm (Lozano et al. 1992). The fluorescence yield ($\sim$0.2%) is limited by an internal molecular process – rapid, nonradiative intersystem crossing from S_1 to T_1, which determines the excited singlet lifetime. Phosphorescence from the triplet state is strongly quenched by molecular collisions (Borge et al. 1990), particularly by molecular oxygen, and is negligible compared to the fluorescence measured with a gated detector using microsecond or less gate times under atmosphere pressure conditions.

A number of properties make LIF of acetone attractive for flow visualization, including: strong signals, short lifetime ($\sim$3 ns) and good linearity with number density and laser pump intensity (Lozano et al. 1992). Practical advantages of acetone include its low cost and low toxicity in comparison to other fluorescent tracers currently available (e.g., nitric oxide and acetaldehyde). Acetone has a molecular weight of 58.08 g/mol and a heat of combustion of 428 kcal/mol. The strong fluorescence signals of acetone allow low seeding levels to be used (e.g., an acetone seeding level of 0.2% by volume was used in the experiment to be presented in Sect. 5); thus, the perturbations to the fuel stream's density and heat of combustion are minimized. The acetone seeding level is limited by its saturation vapor pressure at the gas temperature.

For the application of acetone to nonisothermal flows, such as flames, a consideration is the dependence of acetone fluorescence yield on temperature. Ideally there should be no temperature dependence at all so that acetone fluorescence signal can be interpreted directly as acetone concentration. Indeed, some researchers have observed negligible influence of both temperature and pressure on acetone LIF (Andresen 1993). Using an excitation wavelength of 308 nm, Tait and Greenhalgh (1992) report a significant increase (70%) in the laser-induced emission from acetone with increasing temperature (300 K < T < 700 K) and attribute this behavior to a contribution of emission from non-thermalized, vibrationally-excited triplets which suffer temperature-dependent quenching. The contribution of this emission may vary significantly with the carrier gas composition (Borge et al. 1990). Paul and Clemens (1993) argue that at atmospheric pressure, the quenching of the non-thermalized triplets should be rapid enough that the temperature dependence of the fluorescence yield will be weak. In the present work, this issue was not investigated directly; however, no anomalies were found in the acetone images of the flows studied here that suggest a strong temperature dependency of acetone fluorescence yield.

In combusting flows, the interpretation of acetone as a marker of unburned fuel requires that several additional issues be addressed. Differences in the chemical behavior of acetone and the fuel of interest must be considered. At elevated temperatures acetone pyrolyzes and reacts with combustion radicals such as H, O, OH and CH_3. The extent to which acetone marks the major fuel species is determined by the relative rates of acetone pyrolysis and radical destruction compared to those of the fuel gas. Additionally, differences in the diffusion

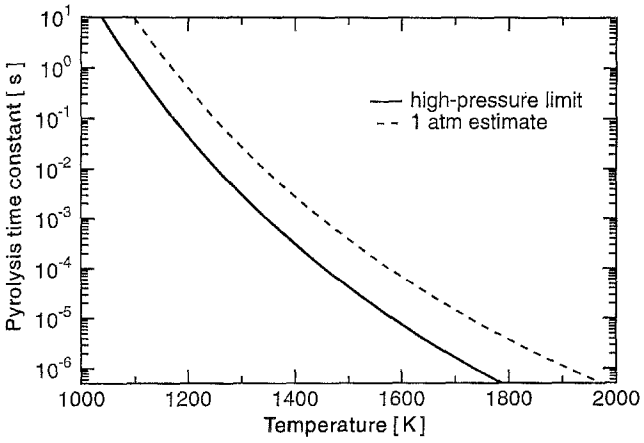

Fig. 1. Acetone pyrolysis time constants as a function of temperature

velocities between acetone and the fuel gas may be important. Each of these issues will be discussed below.

Acetone pyrolyzes by the reaction $CH_3COCH_3 \rightarrow CH_3CO + CH_3$, which is a unimolecular reaction and therefore is a function of pressure as well as temperature. Measurements of this rate, which have been reported for temperatures between 1350 K and 1650 K and for number densities less than 10^{-3} mol/cm^3 (Ernst et al. 1976), indicate that for number densities less than 10^{-5} mol/cm^3 (corresponding to typical combustion temperatures at 1 atm) the pyrolysis rate is in the fall-off region. Listed in Table 1 are two reaction rate expressions for acetone pyrolysis: the high-pressure limit rate from Ernst et al. and an estimate for the rate at 1 atm based on their data. The time constants associated with each of these pyrolysis rates are shown as a function of temperature in Fig. 1. The pyrolysis rates for hydrogen and methane are negligible compared to that of acetone; thus, application of acetone as a marker of methane and hydrogen is best suited to reacting flows with lower combustion temperatures and short residence times where the effects of pyrolysis will be minimized. The pyrolysis rates of more complicated hydrocarbon fuels, such as ethane and propane, are comparable to that of acetone; thus, pyrolysis may present less of a complication in these flows. In the present work, only the application of acetone to methane and hydrogen flames will be considered.

Radical attack on acetone is characterized by the general hydrogen atom abstraction reaction $R + CH_3COCH_3 \rightarrow RH + CH_2COCH_3$, where R represents a radical species. Measured reaction rate coefficients for attack by H (Ambridge et al. 1976), O (Herron 1988), OH (Atkinson et al. 1989) and CH_3 (Shapiro and Weston 1972) are listed in Table 1. Although these radical attack rate coefficients are fits to measurements made at temperatures below 1000 K, extrapolation of these fits to higher temperatures typical of combusting flows is adequate to assess the significance of radical attack on acetone. The rate coefficients for the reactions with H, O and OH are plotted as a function of temperature in Fig. 2. Also plotted in Fig. 2 and listed in Table 1 are the rate coefficients for O and OH attack on hydrogen (Miller and Bowman 1989). Comparison of the H atom removal rates of hydrogen and acetone indicates that all of these rates are within an order of magnitude over the full range of combustion temperatures; thus, the overall rates of

Table 1. Reaction rate coefficients: $k = AT^b \exp(-E_a/RT)$

Reaction	A	b	E_a (kcal/mole)	units
$CH_3COCH_3 \rightarrow CH_3CO + CH_3$				
a) high-pressure limit	2.7×10^{16}	0	81.6	s^{-1}
b) 1 atm estimate	3.0×10^{15}	0	81.6	
$R + CH_3COCH_3 \rightarrow RH + CH_2COCH_3$				
a) R = H	1.86×10^{13}	0	6.36	cm^3/mole/s
b) R = O	1.0×10^{13}	0	5.96	
c) R = OH	1.0×10^{12}	0	1.19	
d) $R = CH_3$	3.24×10^{11}	0	9.63	
$O + H_2 \rightarrow OH + H$	5.06×10^4	2.67	6.29	cm^3/mole/s
$OH + H_2 \rightarrow H_2O + H$	1.17×10^9	1.3	3.63	

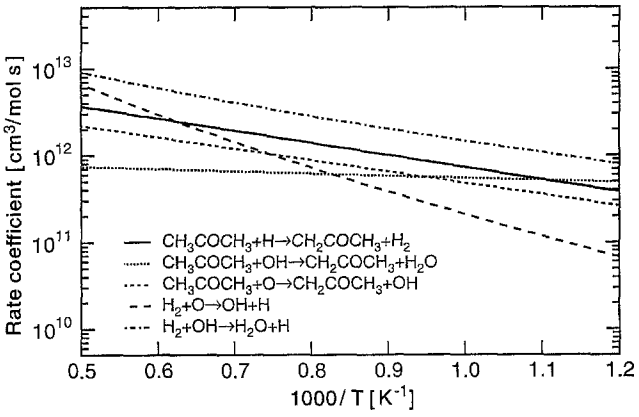

Fig. 2. Reaction rate coefficients for radical attack on acetone and molecular hydrogen as a function of temperature

destruction of acetone and hydrogen by radical attack will be similar. Although not shown, the H atom removal rates of methane and other hydrocarbons by radical attack are similar to that of acetone as well.

Another issue relevant to the discussion of acetone as a marker of fuel gas is the preferential diffusion of the fuel relative to acetone, particularly for light fuels such as methane or hydrogen. In imaging experiments where the goal is to visualize the large-scale structure of the flow, it is usually not possible to resolve the zones of diffusive mixing – the size of which is usually below the resolution of the imaging system. Thus, it is only necessary to consider the effect of preferential diffusion on the composition of the products of combustion. In a turbulent reacting flow, the significance of the effects of preferential diffusion on the rates of consumption of reactants will scale with Damköhler number. For high Damköhler numbers, reactants are consumed predominantly in strained laminar flames; hence, the rates of consumption of reactants and therefore the composition of the combustion products will be sensitive to the effects of preferential diffusion. However, for small Damköhler numbers most of the chemical reaction occurs after the reactants have been molecularly mixed; thus, the composition of the combustion products will be insensitive to the effects of preferential diffusion. Hence, the degree to which the interpretation of acetone signal as a marker of unburned fuel will be complicated by the effects of preferential diffusion will scale with Damköhler number. For heavier hydrocarbon fuels, which have molecular weights closer to that of acetone, the effects of preferential diffusion may not be significant; however, the extent to which differences in the transport properties are important will have to be assessed on a case-by-case basis.

In summary, the interpretation of acetone as a marker of unburned fuel concentration is complicated primarily by two factors: pyrolysis and preferential diffusion. Both of these effects are exacerbated in combusting flows with long residence times and high temperatures (i.e., high Damköhler flows).

3 Experimental apparatus

Acetone's broadband absorption in the UV allows it to be excited by the same laser used to excite OH. Several different pumping schemes, each with its own advantages and disadvantages, have been employed for OH LIF imaging (Seitzman and Hanson 1993); all of these schemes can be used for simultaneous excitation of acetone fluorescence. Figure 3 shows a schematic diagram of the experimental apparatus. For the low-speed experiments (Sect. 4), a Lambda Physik Model 203MSC (Göttingen, Germany) broadband (~0.5 nm) XeCl excimer laser producing up to 300 mJ of energy per pulse at 308 nm was used. A narrow linewidth (~0.01 nm), Lambda Physik Model 150T (Göttingen, Germany) XeCl excimer laser tuned to the $Q_1(3)$ line of the (0, 0) band of the $A^2\Pi^+ \leftarrow X^2\Sigma$ system of OH and producing 100 mJ per pulse was used for the high-speed experiments (Sect. 5).

The large spectral separation between the OH fluorescence, at ultraviolet wavelengths, and the acetone fluorescence, which occurs in the visible spectrum (380–540 nm), allows the use of optical filtering to discriminate between these signals. The fluorescence signals are recorded simultaneously on separate intensified CCD video cameras. The OH camera is equipped with a Schott UG 11 (Duryea, Pennsylvania) color-glass filter to block visible emission, and a 105 mm, $f/4.5$ UV photographic lens (quartz optics). The acetone camera is equipped with a UV-blocking, 50 mm, $f/1.2$ standard glass lens. A 2 μs intensifier gate duration (overlapping the laser pulse) allows LIF signal collection while rejecting natural luminous emission from the flame.

The simultaneous image pairs are acquired with a frame grabber in a PC/AT computer at 8 bits/pixel digital resolution and an effective framing rate of 8 Hz. They are later corrected for

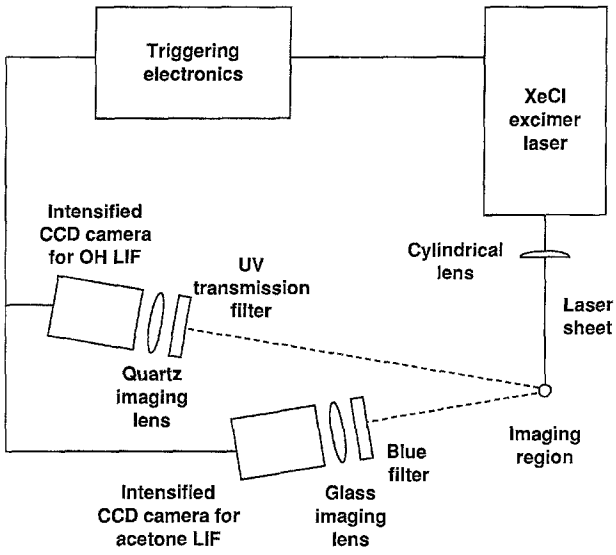

Fig. 3. Experimental setup for OH/acetone planar laser-induced fluorescence imaging

background scattering, nonuniform laser sheet intensity and camera response, as well as for the slightly differing fields of view of the two cameras. Due to the short OH and acetone fluorescence lifetimes, the temporal resolution is determined by the 20 ns laser pulse duration which is sufficient to eliminate any motion blur in the images. The spatial resolution, which is limited by the laser sheet thickness, is roughly 0.3 mm.

4
Low-speed jet flames

Initial development of this imaging technique was carried out in low Reynolds number methane and hydrogen jet diffusion flames using a broadband XeCl excimer laser with maximum pulse energies of 300 mJ. Excellent signals were obtained, but the image interpretation was complicated by a number of factors, most of which are similar to those encountered by Tait and Greenhalgh (1992) who used acetaldehyde as a fuel stream marker under similar conditions. Results from the methane flame experiments are presented to illustrate these effects.

The flame consists of a methane jet diffusion flame in ambient air. The Reynolds number of the fuel jet at the nozzle exit ($d = 2.2$ mm) is 3100. The methane is bubbled through a bath of liquid acetone to produce an acetone seeding level of 10% by volume; the seeding level is determined from Rayleigh scattering measurements. Although this seeding level perturbs the fuel stream density and heat of combustion, which are increased by 26% and 10%, respectively, these effects are tolerable for the purpose of demonstrating the technique.

Figure 4 shows simultaneous acetone and OH LIF images of the acetone-seeded flame. The imaged area is 6.8 cm high and 4.2 cm wide, and the bottom of the images is 3.7 cm (17 nozzle diameters) above the end of the fuel nozzle. The region of the flowfield imaged was chosen because the flame is mostly free of visible soot emission over this range of positions. Based on mean velocity of the fuel jet, the convective time from the fuel nozzle to the bottom of the imaged region is 4.7 ms, and the time to convect across the imaged area is 8.5 ms. These residence times greatly exceed the acetone pyrolysis time constant for the range of combustion temperatures in this flow; thus, significant destruction of acetone by pyrolysis will occur in the hotter regions of the flow. Since methane pyrolysis is much slower than acetone pyrolysis, the acetone fluorescence is not expected to be a good indicator of the methane concentration. Additionally, the Damköhler number for this flow is high due to the high combustion temperatures and low flow velocities; thus, the effects of preferential diffusion on the reactant consumption rates will be significant as well.

As discussed by Tait and Greenhalgh (1992), interferences present in hydrocarbon flames include laser-induced incandescence from soot and LIF from polycyclic aromatic hydrocarbons (PAH's) formed from the products of fuel pyrolysis. These spurious signals can to a large degree be reduced by spectral filtering (a blue glass filter that rejected wavelengths greater than 480 nm was used here), but residual interference can introduce ambiguities in interpreting acetone LIF images. The left image in Fig. 4 shows the visible laser-induced fluorescence. In addition to the strong acetone LIF from the center of the fuel jet, weak emission ($\sim 3\%$ of the maximum acetone fluorescence) due to these sources exists at the limit of detection between the central fuel jet and the regions of OH. This interference probably scales with the acetone seeding here, but in flames burning heavier hydrocarbons, which pyrolyze similarly to acetone, such emission will set a lower limit on the level of acetone seeding required for monitoring the parent fuel concentration.

The centre image of Fig. 4 is the ultraviolet laser-induced emission. The two long, thin regions of OH fluorescence mark the flame reaction zones. Between the two braids of OH fluorescence, a ghost image of the jet is produced by Rayleigh scattering from the methane-acetone fuel mixture. Surrounding the jet, laser scattering from particulates in the unfiltered laboratory air is seen. Without wishing to overemphasize the point (because interpretation is complicated by the unknown response of the particulates to the high-temperature environment), we remark that large regions of low UV emission are evident between the ambient air and the regions of OH fluorescence. A looped structure corresponding to Mie scattering from soot appears at the top of the image, on the fuel-rich side of the right-hand OH braid. A tunable narrowband laser (as used in the experiments of Sect. 5) could be employed to significantly increase the OH LIF signal relative to these interferences.

When the acetone and OH images are overlaid as in the right-hand image of Fig. 4, little correlation between the acetone and OH LIF is seen. A sizable region of almost zero acetone signal appears between the center of the fuel stream and the OH regions, corresponding to the destruction of acetone by pyrolysis. The same effect is seen in low-speed acetone-seeded hydrogen jet flames (e.g., Paul and Clemens 1993). Although the acetone fluorescence does not represent the methane concentration, which will extend closer to the flame zone than the acetone, it does indicate that a significant degree of mixing between the central fuel jet and hot combustion gases is occurring. Additionally, the images show the reaction zones are laminar-like, indicating the flow has locally relaminarized, an effect which has been observed previously in flames at similar Reynolds numbers (e.g., Takagi et al. 1980).

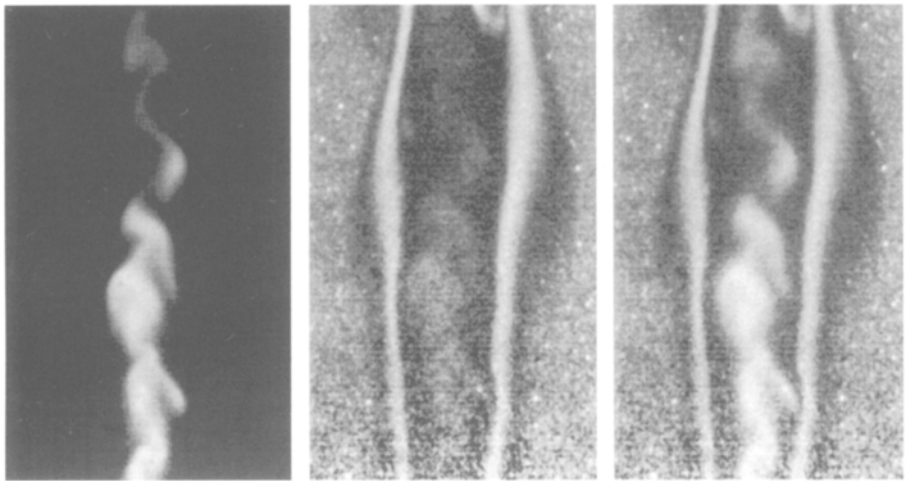

Fig. 4. Simultaneous OH/acetone PLIF images of a methane jet diffusion flame. The fuel jet nozzle is 17 diameters below the bottom of the image; the images are 6.8 cm high and 4.2 cm wide. From left to right, the images show the acetone, OH and overlaid OH and acetone

Table 2. Mixing layer free stream conditions

	Stream 1: oxidizer	Stream 2: fuel
Total temperature (K)	1600	270
Mach number	1.4	0.3
Static temperature (K)	1250	26.5
Velocity (m/s)	970	110
Molar composition	$X_{O_2}=0.23$	$X_{H_2}=0.10$
	$X_{H_2O}=0.25$	$X_{N_2}=0.90$
	$X_{N_2}=0.52$	$X_{CH_3COCH_3}=0.002$
Mass flowrate (kg/s)	0.60	0.45
	Static pressure = 0.88 atm	

In summary, the OH/acetone imaging technique is not well-suited for studying low-speed flames where the fuel has a very different pyrolysis rate and diffusion velocity than that of acetone (e.g., methane and hydrogen). This technique may find application in flames burning heavier hydrocarbon fuels which pyrolyze and diffuse similarly to acetone; however, in these flames, interferences from laser-induced incandescence of soot and fluorescence of polycyclic aromatic hydrocarbons may present significant difficulties for this technique as they do for other laser-based visualization methods.

5
Supersonic reacting mixing layer

Experiments were also performed in a large-scale, blowdown flow facility which produces a plane mixing layer between a supersonic, high-temperature, oxidizing stream and a subsonic, ambient-temperature, fuel stream (Miller et al. 1993). The high-temperature, oxidizing stream is produced by burning oxygen-enriched air and hydrogen in a vitiation heater and expanding the combustion products through a supersonic nozzle. The vitiation heater is operated fuel-lean; thus, the major products of combustion are oxygen, water vapor and nitrogen. The fuel stream consists of hydrogen diluted with nitrogen. For imaging purposes, acetone is seeded into the fuel stream by spraying liquid acetone through a fine atomizing spray nozzle which produces droplet diameters below 100 microns. Subsequently, the acetone droplets evaporate in the flow system prior to entering the test section. The test section measures 8 cm by 10 cm in cross-section and 45 cm in length, with uncooled quartz windows providing full optical access for most of its length.

Table 2 lists the mixing layer free stream conditions for the results presented here. The mixing layer Reynolds number, defined as $Re=(U_1-U_2)\,\delta/\nu$, where U_1 and U_2 are the high- and low-speed free stream velocities, respectively, δ is the width of the mixing layer and ν is the average kinematic viscosity, is approximately 370,000 at the imaging position. The fuel stream acetone seeding level is 2000 ppm, which represents a compromise between the desire to minimize the perturbation to the flow and to maximize the signal-to-noise ratio in the acetone images. This seeding level ($\sim$1 Torr) is well below the saturation vapor pressure of acetone at the fuel stream static temperature (40 Torr at 265 K). Addition of acetone to the fuel stream has a negligible effect ($<$1%) on its density; however, the heat of combustion of the fuel stream mixture and the overall fuel-to-air ratio of the mixing layer both increase by about 15%. While these effects are not negligible, they do not interfere with the goals of the experiment.

A representative selection of simultaneous OH/acetone PLIF images of the mixing layer in side-view are shown in Fig. 5. The digital images (300 × 233 pixels) correspond to a region 7 cm wide by 5 cm tall, centered 22 cm downstream of the splitter tip.

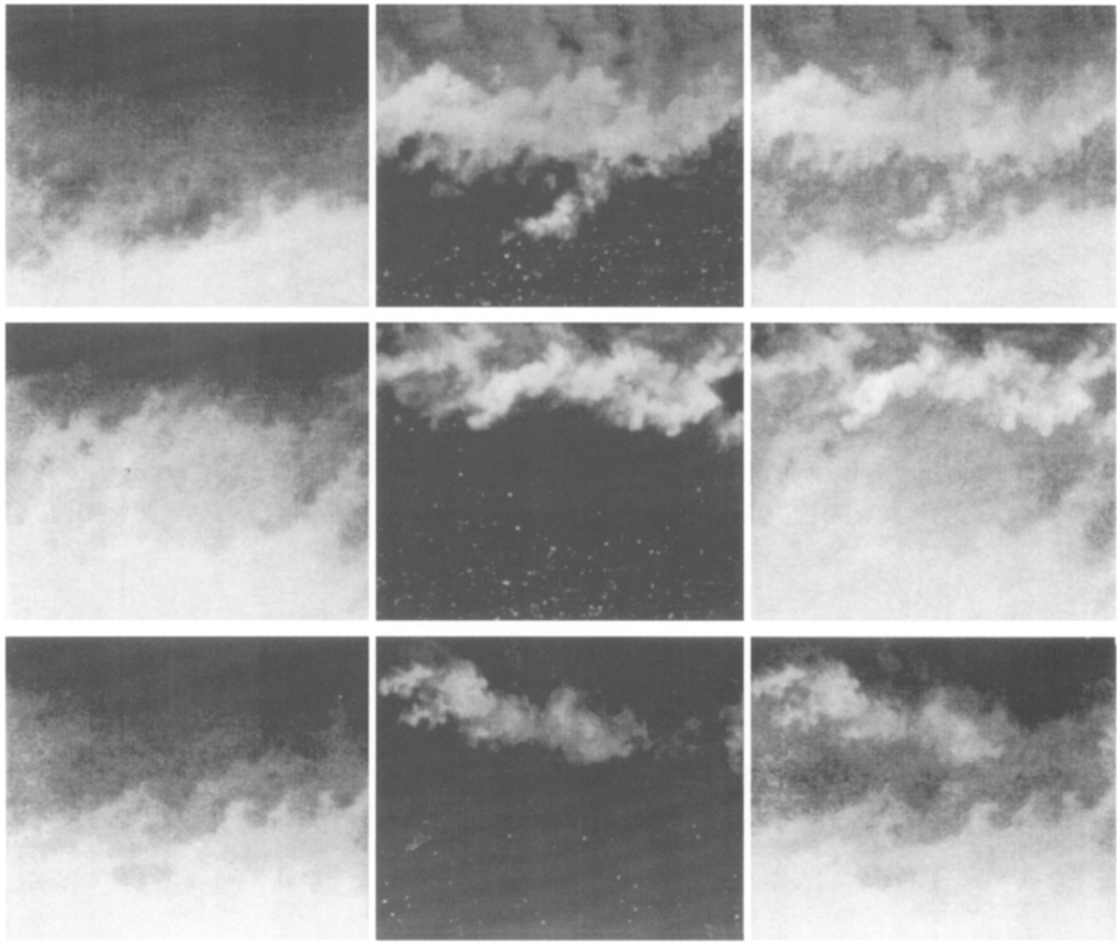

Fig. 5. Three simultaneous OH/acetone PLIF images of the mixing layer in side-view. The flow is left to right; the supersonic vitiated-air stream is on the top, and the subsonic fuel stream is on the bottom. The image size is 7 cm wide by 5 cm high, and the center of the image is 22 cm downstream of the splitter tip. From left to right, the images show the acetone, OH and overlaid OH and acetone

The average convective time from the splitter tip to the imaging station is about 0.5 ms, and the convective time across the imaged area is 140 μs. The pyrolysis time constant at 1 atm and 1250 K, which is the maximum temperature in the mixing layer (Miller et al. 1993), is about 50 ms. Comparing this time with the residence times indicates the pyrolysis is not a significant mechanism for acetone destruction in the mixing layer. Additionally, estimates of the chemical times for product formation in the mixing layer indicate that the overall Damköhler number of the mixing layer is about unity (Miller et al. 1993). The discussion of the scaling of preferential diffusion effects with Damköhler number presented previously suggests that the effects of preferential diffusion will not be significant in this flow. These results indicate that acetone is a reasonable marker of unburned hydrogen in the mixing layer.

The peak signal-to-noise ratio, based on root-mean-squared noise levels, is about fifteen for both OH and acetone images. Attenuation of the laser beam was not observed, which is consistent with the estimated optical depth of the OH and acetone regions of the flow. Some radiative trapping of the emitted OH fluorescence may occur due to the depth of the reacting layer between the detector and the laser-illuminated plane. A small number of unvaporized acetone droplets, which elastically scattered the laser light, are seen as small, bright points in the OH images. This problem arose because in the present configuration, the acetone seeding station could not be placed sufficiently far upstream of the test section for complete vaporization of all droplets. The droplets cannot be discerned in the acetone images, implying that their size and number density are small. Since they are confined to the low speed stream and rarely appear in the mixing layer, the acetone droplets do not affect the results of this experiment.

In the acetone images, the region of maximum signal level at the bottom of the frame corresponds to the fuel stream, where the acetone was initially seeded. Regions of lower signal correspond to fluid from the fuel stream which has been entrained into the mixing layer; the lower acetone signal levels result from dilution by and chemical reaction with existing fluid in the mixing layer. The boundary between the region of maximum acetone signal (fuel stream) and the region of lower acetone signals (mixing layer) represents the instantaneous position of the lower edge of the mixing layer. Based on the previous discussion of acetone behavior in high temperature environments, the amount of unburned hydrogen at a given

point scales with the acetone signal at that point. Although acetone is not a conserved scalar, different signal levels necessarily indicate different mixture compositions; thus, higher acetone signals mark the cooler regions of the mixing layer rich in fuel-stream fluid, and lower acetone signals indicate hotter regions of the mixing layer rich in oxidizing-stream fluid and combustion products.

In the OH images, the signal is limited primarily to a region adjacent to the high-temperature stream; the upper edge of the mixing layer coincides with the upper edge of the OH signal. Residual OH from the vitiation heater is visible in the high-temperature stream in some of the images. Based on the measured detection sensitivity of the imaging system, the peak OH levels in the images are estimated to be between one and two orders of magnitude greater than equilibrium, indicating significant OH production in the mixing layer.

Although the instantaneous appearance of the images varies, all of the images show that high acetone signals and OH signals are mutually exclusive, indicating that regions of OH and regions of high acetone concentration have distinctly different mixture fractions. This observation suggests that the mixing layer is comprised primarily of two zones: a hot, combusting zone containing OH and a cooler, nonreacting zone containing unburned fuel. The structural features of the reacting mixing layer seen in these images are similar to those of nonreacting mixing layers at similar compressibilities (Clemens and Mungal 1992), supporting the present interpretation of the acetone and OH signals. The relatively low combustion temperatures and short residence times in this flow allow the interpretation of acetone as a marker of unburned hydrogen.

6
Conclusion

A simple two-camera PLIF imaging technique for simultaneous visualization of OH radicals and unburned fuel in turbulent reacting flows has been developed. In this technique, OH and acetone laser-induced fluorescence are excited simultaneously by a single pulse from an ultraviolet laser and are imaged separately on two intensified cameras. For combusting flows in which the primary fuel is hydrogen or methane, analysis of the chemical behaviour of acetone indicates that the interpretation of acetone as a marker of unburned fuel is complicated primarily by two factors: pyrolysis and preferential diffusion. Both of these effects are exacerbated in flows with long residence times and high temperatures. The imaging technique was applied to a low Reynolds number methane-air diffusion flame and a supersonic, hydrogen-air mixing layer to illustrate the dependence of the signal interpretation on the flow properties. It is concluded that the technique is best suited to high-speed flows with low combustion temperatures (<1600 K) or flames burning heavier hydrocarbon fuels whose chemical behavior and transport properties are similar to that of acetone.

One significant improvement to this technique would be to use nonresonant excitation of OH so that elastic laser scattering can be rejected by optical filtering. In fact, subsequent work in the supersonic combustion tunnel has used a frequency-doubled dye laser (20 mJ at 285 nm) to excite the (1, 0) band of OH with collection of fluorescence from the (0, 0) and (1, 1) bands. The resulting OH and acetone fluorescence signals have been found to be comparable to those obtained in the present work (Miller et al., 1993b).

References

Ambridge PF; Bradley JN; Whitlock DA (1976) Kinetic study of the reactions of hydrogen and oxygen atoms with acetone. J Chem Soc Faraday Trans I, Vol. 72: 1870–1876

Andresen P (1993) Private communication

Arnold A; Becker H; Suntz R; Monkhouse P; Wolfrum J; Maly R; Pfister W (1990) Flame front imaging in an internal-combustion engine simulator by laser-induced fluorescence of acetaldehyde. Opt Lett 15: 831–833

Atkinson R; Baulch DL; Cox RA; Hampson RF Jr.; Kerr JA; Troe J (1989) Evaluated kinetic and photochemical data for atmospheric chemistry: Supplement III. J Phys Chem Ref Data 18, 881

Borge MJG; Figuera JM; Luque J (1990) Study of the emission of the excited acetone vapor at intermediate pressures. Spectrochim. Acta 46A (4): 617–621.

Clemens NT; Mungal MG (1992) Two- and three-dimensional effects in the supersonic mixing layer. AIAA J 30(4): 973–981

Dibble RW; Long MB; Masri A (1986) Two-dimensional imaging of C_2 in turbulent nonpremixed jet flames. Prog Astronaut Aeronaut 105: 99–109.

Ernst J; Spindler K; Wagner HGg (1976) Untersuchungen zum thermischen Zerfall von Acetaldehyd und Aceton. Berichte der Bunsen-Gesellschaft für Physikalische Chemie 80(7): 645–650.

Hanson RK (1988) Combustion diagnostics: planar imaging techniques. Twenty-first Symposium (International) on Combustion/The Combustion Institute, 1677–1691.

Herron JT (1988) Evaluated chemical kinetic data for the reactions of atomic oxygen O(3P) with saturated organic compounds in the gas phase. J Phys Chem Ref Data 17: 967

Long MB; Levin PS; Fourguette DC (1985) Simultaneous two-dimensional mapping of species concentration and temperature in turbulent flames. Opt Lett 10: 267–269

Lozano A; Yip B; Hanson RK (1992) Acetone: a tracer for planar concentration measurements in gaseous flows by planar laser-induced fluorescence. Exps in Fluids 13: 369–376.

Miller JA; Bowman CT (1989) Mechanism and modeling of nitrogen chemistry in combustion. Prog Energy Combust Science 15 (4): 287–338.

Miller MF; Island TC; Yip B; Bowman CT; Mungal MG; Hanson RK (1993a) An experimental study of the structure of a compressible, reacting mixing layer. AIAA paper 93-0345, 31st Aerospace Sciences Meeting, Reno, NV

Miller MF; Island TC; Seitzman JM; Mungal MG; Bowman CT; Hanson RK (1993b) "Compressibility Effects in a Reacting Mixing Layer," AIAA-93-1771, presented at 29th AIAA/SAE/ASME/ASEE Joint Propulsion Conference, Monterey, CA.

Namazian M; Schmitt RL; Long MB (1988) Two-wavelength single laser CH and CH_4 imaging in a lifted turbulent diffusion flame. Appl Opt 27: 3597–3600.

Paul P; Clemens NT (1993) Planar laser-induced fluorescence imaging of lifted H_2-air flames. AIAA paper 93-0800, 31st Aerospace Sciences Meeting, Reno, NV.

Schefer RW; Namazian M; Kelly J (1990) CH, OH and CH_4 concentration measurements in a lifted turbulent-jet flame. Twenty-third Symposium (International) on Combustion/The Combustion Institute, 669–676

Seitzman JM; Hanson RK (1993) Comparison of excitation techniques for quantitative fluorescence imaging of reacting flows. AIAA J 31 (3): 513–519

Shapiro JS; Weston RE Jr. (1972) Kinetic isotope effects in the reaction of methyl radicals with molecular hydrogen. J Phys Chem 76 1669–1679

Tait NP; Greenhalgh DA (1992) 2D laser-induced fluorescence imaging of parent fuel fraction in nonpremixed combustion. Twenty-fourth Symposium (International) on Combustion/The Combustion Institute, 1621–1628.

Takagi T; Shin H; Ishio A (1980) Local laminarization in turbulent diffusion flames. Comb. and Flame 37: 163–170